

Data-Driven Channel Acquisition with Pilot Decontamination in IRS-Aided Communication Systems

Majumder Haider¹, Imtiaz Ahmed¹, Md. Zoheb Hassan², Mohammad Matin³ and Cong Pu⁴

¹Department of Electrical Engineering and Computer Science, Howard University, Washington, DC, USA

²Department of Electrical and Computer Engineering, Université Laval, QC, CA

³Department of Electrical and Computer Engineering, University of Denver, Denver, CO, USA

⁴Department of Computer Science, Oklahoma State University, Stillwater, OK, USA

¹Corresponding author's e-mail: majumder.haider@bison.howard.edu

Abstract—This paper aims to enhance the cascaded channel estimation process of intelligent reflecting surface (IRS)-aided communication systems while considering the detrimental effect of pilot signal contamination. When the transmitter is equipped with massive multiple-input multiple-output (mMIMO) antennas, and the IRS consists of a large number of reflecting elements, it is practically infeasible to allocate orthogonal pilots over each cascaded link, each consisting of a pair of antenna and reflecting elements. Reusing pilot signals over multiple parallel cascaded links causes interference, known as pilot contamination. Severe pilot contamination deteriorates the accuracy of the channel estimation process significantly. Accurate estimation of high-dimensional cascaded channels of IRS is crucial to distribute narrow beams in the desired direction, which becomes even more cumbersome in the presence of pilot contamination. To address this challenge, we propose deep learning-empowered two approaches to accurately estimate the channel gains of the cascaded links. Subsequently, learning from the correlation of the estimated cascaded links, we predict the cascaded links for other reflecting elements. Simulation results demonstrate the improved performance of the proposed techniques over the baseline schemes.

Index Terms—IRS, cascaded channel estimation, pilot contamination, deep learning, B5G.

I. INTRODUCTION

The goal of next-generation mobile communication is to combine human communication with seamless connectivity for machines and objects that make up the Internet of Everything (IoE). Several developing technologies, such as wearable gadgets, virtual/augmented reality, and fully immersive experience (3D) in real-time are influencing human end users' behavior, and they have unique user satisfaction criteria [1]. As a result, these data-hungry use cases push the wireless standards in several areas, including data throughput, latency, reliability, device/network energy efficiency, traffic volume density, mobility, and connection density. The fifth generation (5G) and beyond 5G (B5G) wireless networks envision to greatly facilitate the implementation of such emerging use cases by offering heterogeneous service requirements like enhanced mobile broadband (emBB), massive machine-type communications (mMTCs), and ultra-reliable low-latency communications (URLLCs) [2], [3].

Intelligent Reflecting Surface (IRS) is a cutting-edge technology in the field of wireless communications and signal processing. It is designed to enhance the performance of wireless communication systems, such as 5G and B5G, by optimizing the propagation of electromagnetic waves [4]. IRS consists of a large number of passive reflecting elements (PREs), such as antennas or metasurfaces, which do not have their own power source. Instead, they rely on incident electromagnetic waves from nearby transmitters that possess the ability to adjust the phase and amplitude of reflected waves to direct the signal beam in a desired direction [5]. This adjustment is dynamically controlled based on signal characteristics and system requirements to optimize signal strength and quality at the receiver, leading to improved data rates, reduced latency, and overcoming interference. However, because the IRS does not have an active radio frequency (RF) chain when equipped solely with PREs, the estimation of cascaded channels consisting of the base station (BS)-to-IRS and IRS-to-user equipment (UE) is a challenging task. Moreover, conventional estimation techniques require high computational complexity to estimate the channel coefficients of IRS-aided cascaded channels because of the high dimension of the channel matrix. Accurate knowledge of the channel correlation matrix is also required. Overall, channel estimation for the cascaded channels in an IRS-aided system is a cumbersome task.

In wireless communication systems, pilot signals are reference (known) signals transmitted by the transmitter to execute necessary tasks such as estimating the wireless channel conditions, synchronizing transmitter and receiver clocks, and optimizing beamforming. When nearby transmitters send the same pilot signals at the same time, it causes distortion or interference in identifying channel conditions and inaccurate estimation of channel state information (CSI), leading to severe performance degradation of the communication systems. This phenomenon is known as pilot contamination. The detrimental effect of pilot contamination focusing on massive multiple-input-multiple-output (mMIMO) communication systems has been investigated in [6] - [10], wherein the authors proposed

the design of pilot patterns, the pilot allocation scheme, and the precoding scheme as different solution approaches.

The deep learning (DL) technique is becoming prevalent in diverse fields, including the domain of wireless communications, to solve highly complex non-linear problems at the physical and link layers efficiently by learning from data without the explicit use of feature engineering. Among other contributions, [11] - [13] employed different deep neural networks (DNN) to estimate propagation channels and suppress the effect of pilot contamination in mMIMO systems.

To the best of our knowledge, the effect of pilot contamination in IRS-assisted communication systems has not been addressed using a data-driven approach in the literature yet. This paper investigates the effect of pilot contamination in IRS-aided communication systems and proposes two data-driven approaches to jointly estimate cascaded channels of the IRS while considering the occurrence of pilot contamination. Our proposed schemes consist of two steps. In the estimation step, we estimate channel gains of a set of PREs by sequentially turning on a single PRE. In the prediction step, we predict the channel coefficients of all other PREs leveraging the data-driven learning of the correlations that exist among all the estimated cascaded channel gains. Fully connected DNNs are used to perform the tasks in both steps. The trade-offs in terms of accuracy and computational complexity of the proposed methods are thoroughly investigated. Simulation results reveal the superior performance of the proposed methods and their performance gap over baseline schemes, especially in the range of low signal-to-noise ratio (SNR) values.

The rest of the paper is organized as follows. In Section II, we describe the system model and signal propagation. The proposed DNN-aided channel estimation and prediction with pilot decontamination are illustrated in Section III. Simulation results with numerical evaluations are discussed in section IV. Finally, Section V concludes the paper.

II. SYSTEM MODEL

We consider the scenario of an urban area in the city center, where skyscrapers hinder line of sight (LoS) links in cellular communications. In the near future, skyscrapers in urban areas will be equipped with low-cost, large but lightweight, and easily installable IRS panels [14]. This facilitates the robust propagation of radio signals in the desired direction while reducing the multipath fading effect of radio signals. In Fig. 1, we consider the IRS-aided narrowband downlink wireless transmission system with a BS, IRS panel, and a single UE. It is worth mentioning that the considered model and the proposed channel estimation and prediction schemes can be extended for multi-user scenarios. We assume that the BS is equipped with M antennas, the IRS panel consists of L PREs, and the UE contains a single antenna. The considered system model can operate in both sub-6 GHz and millimeter wave bands. Note that there is no direct link between BS and UE in the considered system due to obstacles; hence, the communication between BS to UE occurs via the IRS. The incident signal at the IRS can independently undergo a phase shift and an amplitude change to each PRE $l \in \{1, 2, \dots, L\}$ of

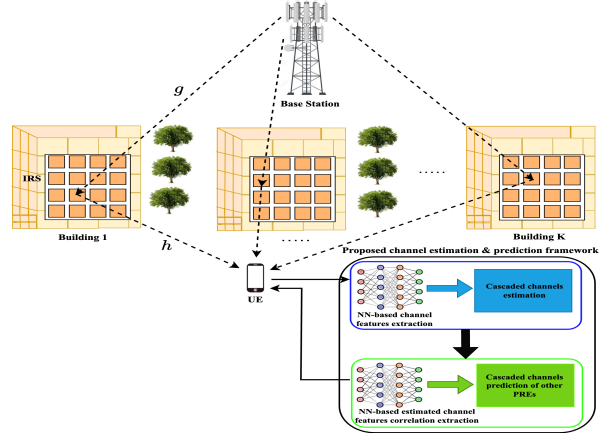


Fig. 1: IRS-aided downlink communication system.

the IRS. The complex reflection coefficient of l th PRE can be denoted as $\phi_l = \beta_l e^{j\alpha_l}$, where the amplitude gain and phase shift of the l th element are represented by $\beta_l \in [0, 1]$ and $\alpha_l \in [0, 2\pi)$, respectively [15]. To increase the strength of the reflected signal and to reduce complexity in cascaded channel estimation, we assume that $\beta_l = 1$ for $l \in \{1, 2, \dots, L\}$. Let us denote the phase shift coefficient matrix as $\Phi = \text{diag}(\phi_1, \phi_2, \dots, \phi_L)$, where $\text{diag}(\cdot, \cdot, \cdot)$ represents the diagonal matrix.

To execute channel estimation, we consider the sequential on-off mode of operation of the PREs for the considered IRS due to its simplicity [4], [15], [16]. Therefore, only one of L PREs is activated at a time to reflect the signal in the desired direction. Since all the reflecting elements are passive, the estimation of the channel from BS to IRS and IRS to UE cannot be computed separately. By turning on one of the PREs of the IRS at a time, the BS-IRS-UE cascaded channels are estimated sequentially. It is assumed that the channels of BS-to-IRS and IRS-to-UE communication links follow independently and identically distributed (i.i.d.) Rician fading, due to the presence of the LoS links with Rice factors $K_{g_{m,l}}$ and K_{h_l} , respectively. Let us assume the BS transmits pilot signals $\mathbf{x}_p \in \mathcal{C}^{1 \times \tau_p}$ of length $\tau_p \geq M$ (in samples), $p \in \{1, 2, \dots, \tau_p\}$ for channel estimation such as

$$\mathbf{x}_{p1}^H \mathbf{x}_{p2} = \begin{cases} \tau_p & p1 = p2 \\ 0 & p1 \neq p2, \end{cases} \quad (1)$$

where $(\cdot)^H$ denotes Hermitian matrix, $p \in \{p1, p2\}$, and $\|\mathbf{x}_p\|^2 = \tau_p$. We incorporate pilot contamination in the considered scenario, denoting $\mathcal{M} < M$ as the number of contaminated pilot sequences. It is worth noting that since the total pilot sequences τ_p do not consist of complete orthogonal pilots, it cannot ensure orthogonal pilot signal transmission for all the transmitter antennas by the BS. The corresponding received signal of the contaminated pilot signal transmission at time t by the UE reflected through the l th PRE can be represented as

$$y_l = \sum_{m \in S_{\mathcal{M}}} \sqrt{\mathcal{P}_m} h_l^* e^{j\phi_l} g_{m,l} x_m + n_l, \quad (2)$$

where S_M denotes a set of transmitter antennas that use the same pilot sequence at the same time. Here, y_l depicts the received signal at UE via l th PRE, \mathcal{P} denotes the transmit power, h_l represents the channel gain between l th PRE of IRS and UE, $g_{m,l}$ signifies the channel gain between BS to IRS, x_m defines the contaminated pilot signal, and n_l depicts the additive white Gaussian noise (AWGN) with zero-mean and unit variance. Here, $(\cdot)^*$ represents a conjugate operation. We denote $\zeta_{m,l} = h_l^* e^{j\phi_l} g_{m,l}$ as the cascaded channel gain associated with the transmit antenna m and PRE l . To estimate $\zeta_{m,l}$, we compute $z_l = y_l x_m^* / \sqrt{M}$ as follows:

$$z_l = \sum_{m \in S_M} \sqrt{\mathcal{P}_m M} \zeta_{m,l} + \frac{n_l x_m^*}{\sqrt{M}}. \quad (3)$$

Our goal is to estimate the cascaded channel $\zeta_{m,l}$ from z_l when PRE $l \in \{1, 2, \dots, L\}$ is turned on. As such, we are required to perform the estimation process sequentially to compute all $\zeta_{m,1}, \zeta_{m,2}, \dots, \zeta_{m,L}$ channels between BS and UE. However, estimating cascaded channels for all L PREs following this on-off sequential approach is a challenging and time-consuming task. Following this urge, we divide our channel gain acquisition process into two steps: a) channel estimation on a selected small number of PREs and b) channel prediction for the remaining PREs based on the estimated channels.

III. DEEP NEURAL NETWORK AIDED ESTIMATION & PREDICTION

In this section, we first describe our proposed two-step (estimation and prediction) data-driven approach to acquire cascaded channels of the considered IRS-aided communication system. We then illustrate the details of the two DNN-empowered methods for both estimation and prediction schemes separately in the following subsections.

A. Two-Step Data-Driven Approach

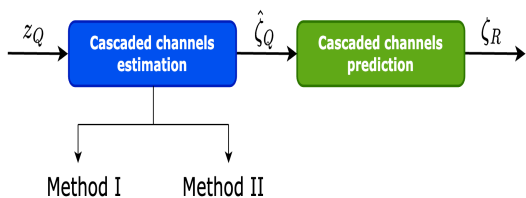


Fig. 2: Proposed two-step data-driven approach.

Fig. 2 illustrates our proposed two-step data-driven approach to acquire (estimation and prediction) the cascaded channel gain. First, we estimate the cascaded IRS channels for $Q \ll L$ number of PREs using one of the two proposed methods, Method I and Method II. Following the estimated cascaded channel gains of Q number of PREs, we predict the remaining $R = L - Q$ number of PREs. The idea of employing a two-step data-driven approach is twofold. Firstly, the IRS panel is usually equipped with a large number of PREs. These PREs are closely embedded in the IRS panel, hence their

inherent signal properties are closely correlated. Secondly, it is computationally burdensome for the transceiver to accurately estimate the cascaded channels for each PRE, especially in the case of a downlink communication system due to the limited resources and energy-constrained hardware of the UE. As such, we leverage data-driven approaches to design channel acquisition schemes that exhibit low computational complexity in real-time data transmission. First, we propose two data-driven estimation schemes that can address pilot contamination and estimate channels for a small number of PREs. Second, another data-driven prediction scheme can learn the underlying correlations among PREs and hence can predict channels for the remaining large number of PREs from the estimated small number of PREs.

B. Cascaded Channels Estimation

We propose two DNN-aided channel estimation schemes, Method I and Method II. While Method I yields lower computational complexity, Method II applies the successive pilot contamination cancellation strategy to improve the performance at the expense of higher complexity.

1) Method I: In this method, the input features of the neural network (NN) model consist of $\mathcal{R}\{z_l\}$ and $\mathcal{I}\{z_l\}$, where \mathcal{R} and \mathcal{I} denote the real and imaginary parts of a complex variable, respectively. The corresponding output labels of the NN model are the cascaded channel for PRE $l \in \{1, 2, \dots, L\}$ and transmit antenna $m \in \{1, 2, \dots, M\}$ that shares the same pilot sequence. The output labels are represented as $[\mathcal{R}\{\hat{\zeta}_{1,l}\}, \mathcal{I}\{\hat{\zeta}_{1,l}\}, \dots, \mathcal{R}\{\hat{\zeta}_{M,l}\}, \mathcal{I}\{\hat{\zeta}_{M,l}\}]$. The NN model is depicted in Fig. 3.

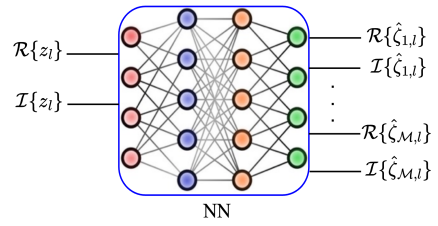


Fig. 3: Neural Network for Method I.

2) Method II: In this approach, the concept of successive interference cancellation (SIC) technique is implemented utilizing DNN [17]. We employ the idea of the SIC decoding technique to minimize pilot contamination using the knowledge of transmit antennas that share the same pilot signal. In this estimation method, D NN models are designed and trained to cancel the impact of $M - 1$ contaminating pilot signals. We set $D = C(S_M)$, where C represents the cardinality of a set. As shown in Fig. 4, the first NN model takes $\mathcal{R}\{z_l\}$ and $\mathcal{I}\{z_l\}$ as the input features to estimate $\mathcal{R}\{\hat{\zeta}_{1,l}\}$ and $\mathcal{I}\{\hat{\zeta}_{1,l}\}$ at the output. The second NN model are fed with the input features $\mathcal{R}\{z_l\} - \mathcal{R}\{\hat{\zeta}_{1,l}\}$ and $\mathcal{I}\{z_l\} - \mathcal{I}\{\hat{\zeta}_{1,l}\}$ to generate the output $\mathcal{R}\{\hat{\zeta}_{2,l}\}$ and $\mathcal{I}\{\hat{\zeta}_{2,l}\}$. Following this sequence the D th NN model is given $\mathcal{R}\{z_l\} - \sum_{d=1}^{D-1} \mathcal{R}\{\hat{\zeta}_{d,l}\}$ and $\mathcal{I}\{z_l\} - \sum_{d=1}^{D-1} \mathcal{I}\{\hat{\zeta}_{d,l}\}$ as input to estimate $\mathcal{R}\{\hat{\zeta}_{D,l}\}$ and $\mathcal{I}\{\hat{\zeta}_{D,l}\}$ as the output.

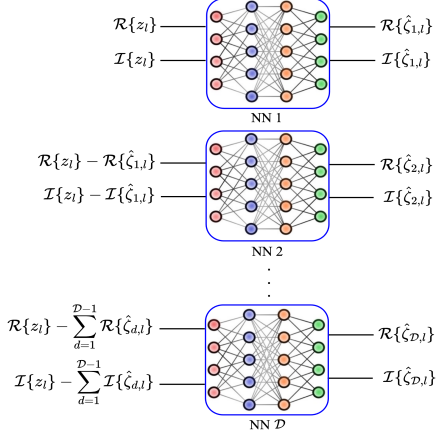


Fig. 4: Neural Network for Method II.

C. Cascaded Channels Prediction

Using Methods I and II first, we compute the cascaded channels of IRS for Q number of PREs. We then feed another fully connected feedforward NN with Q estimated cascaded channel gain to predict the remaining channel gains for R number of PREs. Refer to Fig. 5, the input features and the corresponding output for the prediction operation can be represented as $\mathcal{R}\{\hat{\zeta}_{M,1}\}$, $\mathcal{I}\{\hat{\zeta}_{M,1}\}$, \dots , $\mathcal{R}\{\hat{\zeta}_{M,Q}\}$, $\mathcal{I}\{\hat{\zeta}_{M,Q}\}$, and $\mathcal{R}\{\hat{\zeta}_{M,Q+1}\}$, $\mathcal{I}\{\hat{\zeta}_{M,Q+1}\}$, \dots , $\mathcal{R}\{\hat{\zeta}_{M,Q+R}\}$, $\mathcal{I}\{\hat{\zeta}_{M,Q+R}\}$ respectively.

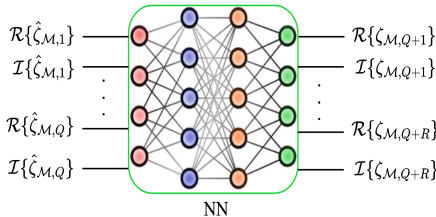


Fig. 5: Neural Network for Prediction.

D. Offline Training and Online Testing (Method I & Method II)

The NN models of Methods I and II are designed with multiple fully connected DNN layers. The first layer is the input layer integrated with the input features followed by G hidden layers. Each hidden layer $g \in \{1, 2, \dots, G\}$ consists of N_g neurons. The last hidden layer G is followed by the final output regression layer. The NN model is trained with U epochs, where each epoch contains V batches of data collected from the training dataset. It is worth pointing out that the training dataset contains data collected over a wide range of SNR. Once trained, the inference model is ready for the online acquisition of cascaded channels while performing the estimation and prediction tasks sequentially.

E. Computational Complexity

The computational complexity for forward and backward propagation in the offline training phase

of Method I and Method II are computed as $\mathcal{O}\left(2L\left(2N_1 + 2mN_G + \sum_{g=2}^G N_{g-1}N_g\right)UV\right)$ and $\mathcal{O}\left(2DL\left(2N_1 + 2N_G + \sum_{g=2}^G N_{g-1}N_g\right)UV\right)$, respectively. On the other hand, the computational complexity in the online testing phase belongs to only forward propagation, hence, the complexity for Method I and Method II can be represented as $\mathcal{O}\left(L\left(2N_1 + 2mN_G + \sum_{g=2}^G N_{g-1}N_g\right)\right)$ and $\mathcal{O}\left(DL\left(2N_1 + 2N_G + \sum_{g=2}^G N_{g-1}N_g\right)\right)$, respectively. In the sequential on-off mode of IRS, the computational complexity of the DNN model is linearly incremental with the increase of L for both training and testing phases, since only one PRE is turned on at a time.

IV. SIMULATION RESULTS

In this section, we first describe the baseline schemes and then discuss the numerical performance evaluations of the proposed DNN-based channel acquisition scheme along with the baseline schemes. It is worth mentioning that the cascaded channel of the BS-IRS-UE link results in a non-Gaussian distribution. Hence, obtaining the optimal minimum mean square error (MMSE) scheme requires the calculation of multidimensional integration and hence is not straightforward to implement in practice [18].

A. Baseline Estimation Schemes

1) *Least Square Estimation (LSE)*: We consider the conventional least squares estimate (LSE) approach as one of the baseline schemes that do not require statistical knowledge of the channel profile. The estimated cascaded channels of the IRS using the LSE method can be expressed as

$$\hat{\zeta}_{m,l} = \frac{z_l}{\sqrt{\mathcal{P}_m \mathcal{M}}}. \quad (4)$$

2) *Convolutional Neural Network (CNN)*: Convolutional Neural Network (CNN) aided channel estimation scheme is considered as another baseline approach. Taking into account the size of the input features of the cascaded channel estimation process, we designed and trained a one-dimensional (1D) CNN to extract spatial correlations. The first layer of the network consists of a sequential input layer. The five middle layers are the core layers, where most computations and learning occur. Each stack of middle layers consists of a one-dimensional convolution (Conv1D) layer, batch normalization layer, and rectified linear unit (ReLU) activation layer. The final layer is the fully connected output layer.

B. Baseline Prediction Schemes

1) *Linear Regression*: In the prediction stage, we consider machine learning (ML) incorporated linear regression as a baseline scheme that yields low computational complexity in predicting cascaded channels from the estimated channels.

C. Numerical Performance Comparison

We demonstrate the numerical results of the proposed DNN-aided channel acquisition frameworks and compare their performance with the considered baseline schemes in this subsection. We adopt normalized mean square error (NMSE) as

a metric to evaluate the performance of the proposed methods in both estimation and prediction tasks. The NMSE can be defined as $\text{NMSE} = \mathbb{E}\left\{\frac{\|\mathcal{Q} - \hat{\mathcal{Q}}\|^2}{\|\mathcal{Q}\|^2}\right\}$. Here, $\mathbb{E}\{\cdot\}$ represents the statistical expectation operation. Moreover, $\mathcal{Q} \in \{s_m\}$ and $\hat{\mathcal{Q}} \in \{\hat{s}_m\}$ denote the actual and the estimated signals, respectively. We set the average SNR as $\gamma = \mathcal{P}_m \mathbb{E}\{|\zeta_{m,l}|^2\}/\sigma_n^2$, where σ_n^2 denotes the noise power spectral density at UE. We leverage the MATLAB DL toolbox [19] for the dataset generation, training, and testing to evaluate the performance of the proposed schemes. We consider 20,000 realizations for training and 6,000 realizations for testing for both the proposed and baseline schemes. For all the demonstrated results, we consider $K_{g_{m,l}} = K_{h_l} = 10\text{dB}$, $M = 8$, $L = 2^a$, $a = 4$, $\mathcal{M} = \mathcal{D} = 3$, $\mathcal{G} = 3$, $N_g = 300$, $Q = 4$, $j = 8$, $U = 100$, and $V = 50$, unless otherwise stated to conduct the simulations.

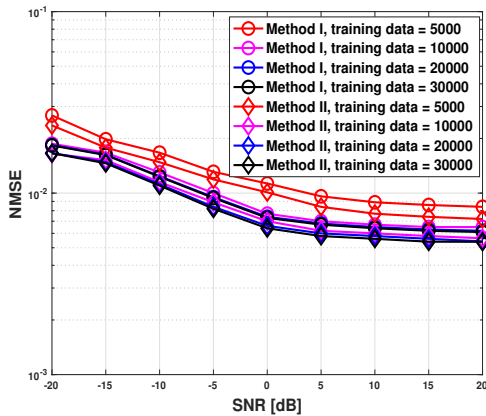


Fig. 6: Training impact on estimation.

Impact of Training Dataset on Estimation: In Fig. 6, we illustrate the impact of the number of training samples on the NMSE across a range of SNR for both proposed Methods I and II during the estimation process. Different configurations of training parameters are considered by varying the cardinality of the training datasets. It is observed that an increase in SNR for a given training dataset decreases NMSE. Moreover, enlarging the dataset size further reduces the NMSE at a fixed SNR. However, the improvement in NMSE performance when increasing the dataset cardinality from 20,000 to 30,000 is relatively marginal compared to the enhancement observed when expanding the dataset size from 5,000 to 10,000. This trend in NMSE performance as a function of dataset size suggests that an optimal selection of training symbols should consider the trade-off between increased training computational complexity and time versus performance gains.

Performance of Proposed Estimation Schemes: Fig. 7 compares the performances of the proposed cascaded channel estimation schemes with those of the baseline schemes. A large gap in estimation error is evident between the LSE and the proposed methods, especially in the low SNR region. Increasing the value of SNR decreases the difference in NMSE between the LSE and the proposed methods. It is observed that the NMSE performance of fully connected feed-forward

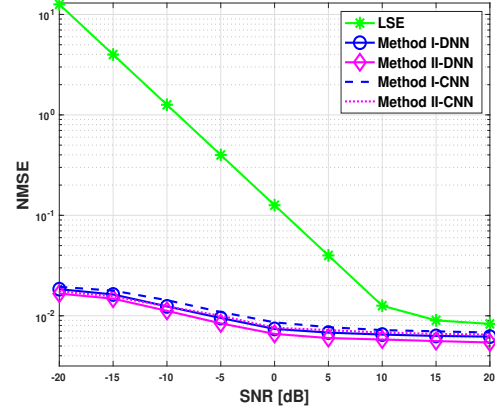


Fig. 7: Cascaded channels estimation error.

DNN is relatively better than the CNN over the entire range of SNR. However, Method II shows lower NMSE compared to Method I in estimating the cascaded channels at the expense of deploying multiple NNs. Therefore, the trade-off between the proposed methods can be optimized intelligently while considering the application requirements, computational resource availability, users' demands, and cellular traffic loads.

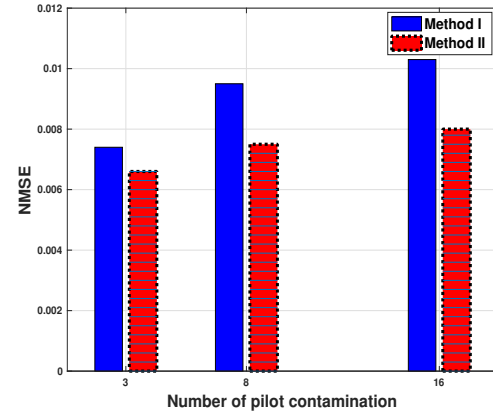


Fig. 8: Effect of increasing pilot contamination.

Fig. 8 illustrates the impact of the variation in the number of pilot contamination on the NMSE for both the proposed estimation methods. We see as the pilot contamination increases the NMSE also increments while anticipating a fixed number of transmitter antennas $M = 128$. Moreover, the gap in NMSE between method I and method II increases with the increasing number of pilot contamination.

Impact of Training Samples on Prediction: Fig. 9 shows the influence of training samples on NMSE while predicting the cascaded channels of the PREs. The figure shows that the NMSE falls sharply when the number of training samples increases to 6000. However, increasing the training samples beyond 6000 makes the decreasing rate of the NMSE significantly low.

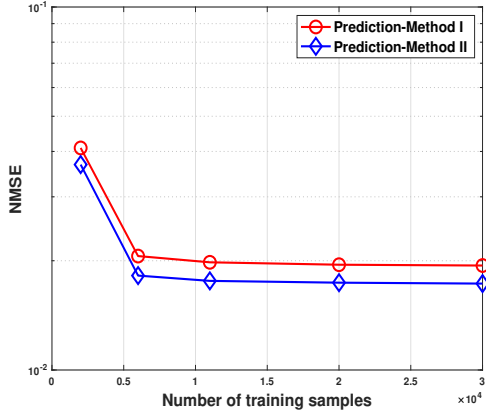


Fig. 9: Training impact on prediction.

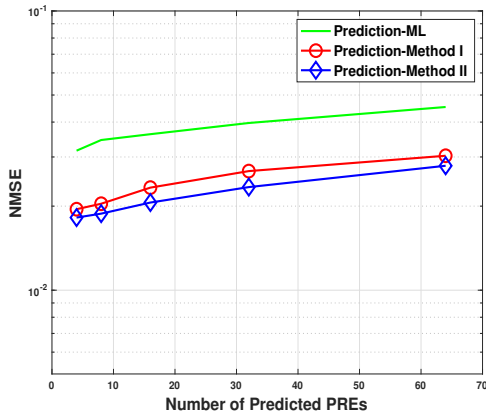


Fig. 10: PREs cascaded channels prediction error.

Performance of Prediction Schemes: Fig. 10 depicts the comparison of cascaded channels prediction error between the proposed methods and the ML integrated linear regression as a baseline scheme. It shows that both the proposed methods outperform the baseline scheme in terms of NMSE noticeably. Moreover, we observe that keeping fixed the number of PREs estimated cascaded channels gain as input features, the prediction NMSE increases slowly while predicting the cascaded channels of the increasing number of PREs. Method II shows lower NMSE than method I in the prediction stage as well.

V. CONCLUSION

This paper investigates the challenging problem of the cascaded channel acquisition for IRS-aided communication systems while addressing the detrimental effect of pilot contamination. We propose a two-step twin DNN framework to address this challenge. The proposed two methods can render notably lower estimation error than the conventional statistical estimation approach, especially in the low SNR region, as well as predict the cascaded channels gain with reasonable accuracy by learning the spatial correlation of the estimated channel of the PREs. In future work, we will analyze customized DNN models, especially considering the inherent structure of the

signal to provide further improved performance in both the estimation and prediction process.

REFERENCES

- [1] F. Hu, Y. Deng, H. Zhou, T. H. Jung, C. -B. Chae and A. H. Aghvami, "A Vision of an XR-Aided Teleoperation System toward 5G/B5G," in *IEEE Communications Magazine*, vol. 59, no. 1, pp. 34-40, January 2021.
- [2] P. Popovski, K. F. Trillingsgaard, O. Simeone and G. Durisi, "5G Wireless Network Slicing for eMBB, URLLC, and mMTC: A Communication-Theoretic View," in *IEEE Access*, vol. 6, pp. 55765-55779, 2018.
- [3] S. R. Pokhrel, J. Ding, J. Park, O.-S. Park, and J. Choi, "Towards enabling critical mMTC: A review of URLLC within mMTC," *IEEE Access*, vol. 8, pp. 131796-131813, 2020.
- [4] Q. Wu, S. Zhang, B. Zheng, C. You and R. Zhang, "Intelligent Reflecting Surface-Aided Wireless Communications: A Tutorial," in *IEEE Transactions on Communications*, vol. 69, no. 5, pp. 3313-3351, May 2021.
- [5] Ö. Özdogan, E. Björnson and E. G. Larsson, "Intelligent Reflecting Surfaces: Physics, Propagation, and Pathloss Modeling," in *IEEE Wireless Communications Letters*, vol. 9, no. 5, pp. 581-585, May 2020.
- [6] H. H. Yang, G. Geraci, T. Q. S. Quek and J. G. Andrews, "Cell-Edge-Aware Precoding for Downlink Massive MIMO Cellular Networks," in *IEEE Transactions on Signal Processing*, vol. 65, no. 13, pp. 3344-3358, July, 2017.
- [7] Z. Zhou, D. Wang and Z. Wang, "Asynchronous pilots scheduling in massive MIMO systems," in *2017 IEEE International Conference on Communications (ICC)*, Paris, France, 2017.
- [8] L. S. Muppireddy, T. Charalambous, J. Karout, G. Fodor and H. Wymeersch, "Location-Aided Pilot Contamination Avoidance for Massive MIMO Systems," in *IEEE Transactions on Wireless Communications*, vol. 17, no. 4, pp. 2662-2674, April 2018.
- [9] X. Zhu, Z. Wang, L. Dai and C. Qian, "Smart Pilot Assignment for Massive MIMO," in *IEEE Communications Letters*, vol. 19, no. 9, pp. 1644-1647, Sept. 2015.
- [10] O. Elijah, C. Y. Leow, T. A. Rahman, S. Nunoo, and S. Z. Iliya, "A comprehensive survey of pilot contamination in massive MIMO-5G system," *IEEE Commun. Surv. Tuts.*, vol. 18, no. 2, pp. 905-923, Apr.-Jun. 2016.
- [11] H. Hirose, T. Ohtsuki and G. Gui, "Deep Learning-Based Channel Estimation for Massive MIMO Systems With Pilot Contamination," in *IEEE Open Journal of Vehicular Technology*, vol. 2, pp. 67-77, 2021.
- [12] B. Lim, W. J. Yun, J. Kim and Y. -C. Ko, "Joint Pilot Design and Channel Estimation Using Deep Residual Learning for Multi-Cell Massive MIMO Under Hardware Impairments," in *IEEE Transactions on Vehicular Technology*, vol. 71, no. 7, pp. 7599-7612, July 2022.
- [13] I. Ahmed, M. Z. Hasan, A. Rubaai, K. Hasan, C. Pu and J. H. Reed, "Deep Learning Assisted Channel Estimation for Cell-Free Distributed MIMO Networks," in *2023 19th International Conference on Wireless and Mobile Computing, Networking and Communications (WiMob)*, pp. 344-349, Montreal, QC, Canada, 2023.
- [14] C. Pan et al., "Reconfigurable Intelligent Surfaces for 6G Systems: Principles, Applications, and Research Directions," in *IEEE Communications Magazine*, vol. 59, no. 6, pp. 14-20, June 2021.
- [15] M. Haider, I. Ahmed, A. Rubaai, C. Pu and D. B. Rawat, "GAN-based Channel Estimation for IRS-aided Communication Systems," in *IEEE Transactions on Vehicular Technology*, doi: 10.1109/TVT.2023.3336601.
- [16] D. Mishra and H. Johansson, "Channel Estimation and Low-complexity Beamforming Design for Passive Intelligent Surface Assisted MISO Wireless Energy Transfer," in *2019 IEEE International Conference on Acoustics, Speech and Signal Processing (ICASSP)*, pp. 4659-4663, Brighton, UK, 2019.
- [17] S. Verdu, "Multiuser Detection," in Cambridge University Press, 1998.
- [18] C. Liu, X. Liu, D. W. K. Ng and J. Yuan, "Deep Residual Learning for Channel Estimation in Intelligent Reflecting Surface-Assisted Multi-User Communications," in *IEEE Trans. on Wireless Communications*, vol. 21, no. 2, pp. 898-912, Feb. 2022.
- [19] MATLAB, "Deep Learning Toolbox," accessed Nov 1, 2023, on <https://www.mathworks.com/help/deeplearning/index.html>.